Cellular/Molecular

PKC-Induced Intracellular Trafficking of Ca_V2 Precedes Its Rapid Recruitment to the Plasma Membrane

Yalan Zhang,[1] Jessica S. Helm,[2] Adriano Senatore,[3] J. David Spafford,[3] Leonard K. Kaczmarek,[1] and Elizabeth A. Jonas[2]

[1]Department of Pharmacology and [2]Department of Internal Medicine, Section of Endocrinology, Yale School of Medicine, New Haven, Connecticut 06520, and [3]Department of Biology, University of Waterloo, Waterloo, Ontario, Canada N2L 3G1

Activation of protein kinase C (PKC) potentiates secretion in *Aplysia* peptidergic neurons, in part by inducing new sites for peptide release at growth cone terminals. The mechanisms by which ion channels are trafficked to such sites are, however, not well understood. We now show that PKC activation rapidly recruits new Ca_V2 subunits to the plasma membrane, and that recruitment is blocked by latrunculin B, an inhibitor of actin polymerization. In contrast, inhibition of microtubule polymerization selectively prevents the appearance of Ca_V2 subunits only at the distal edge of the growth cone. In resting neurons, Ca_V2-containing organelles reside in the central region of growth cones, but are absent from distal lamellipodia. After activation of PKC, these organelles are transported on microtubules to the lamellipodium. The ability to traffic to the most distal sites of channel insertion inside the lamellipodium does, therefore, not require intact actin but requires intact microtubules. Only after activation of PKC do Ca_V2 channels associate with actin and undergo insertion into the plasma membrane.

Key words: **calcium channel; PKC; actin; microtubule; growth cone; *Aplysia***

Introduction

Changes in neuronal excitability and neurotransmitter release regulated by protein kinases underlie many prolonged changes in behavior (Baines, 2003; Emoto et al., 2004; Fadool et al., 2004; Lin et al., 2004). An example of this occurs in bag cell neurons (BCNs) of *Aplysia californica*, which, in response to brief stimulation, undergo long-lasting changes in excitability and secretion that alter reproductive behaviors (Conn and Kaczmarek, 1989). These changes are caused by activation of protein kinases that modulate ion currents, enlarge secretory endings and cause movement of secretory granules to sites adjacent to calcium channels, in preparation for neuropeptide release (Kaczmarek et al., 1980; Azhderian and Kaczmarek, 1990; Fisher and Kaczmarek, 1990; Wilson and Kaczmarek, 1993; Jonas et al., 1997; Wayne et al., 1999).

One component of the response of BCNs to stimulation is the activation of protein kinase C (PKC) (DeRiemer et al., 1985; Strong et al., 1987; White et al., 1998). This enzyme rapidly increases calcium current and expands growth cones, which, after coactivation of other kinases, become secretory endings packed with neuropeptide granules (Forscher et al., 1987; Knox et al., 1992). BCNs contain two physiologically characterized calcium channels (Ca_V1, Ca_V2), one of which (Ca_V2) is normally localized to intracellular vesicles and is sensitive to PKC (White et al., 1998). Activation of PKC with phorbol esters or diacylglycerols rapidly and reproducibly enhances voltage dependent calcium current by twofold to threefold (DeRiemer et al., 1985; Strong et al., 1987; Jonas et al., 1996).

In channel recordings at the soma, the increase in current produced by activation of PKC is associated with the appearance of a new 24 pS calcium conductance (Strong et al., 1987). Ca_V2 is normally located intracellularly throughout the soma and in the central region of growth cones (White and Kaczmarek, 1997). Previous work has suggested that enhancement of calcium current could result from translocation of intracellular Ca_V2 into the plasma membrane at the soma and the distal edge of growth cones. Fura-2 calcium imaging showed that activation of PKC produces new sites of calcium entry in BCNs at the very distal tips of neurites (Knox et al., 1992), where neuropeptide secretion is believed to occur (Tulsi and Coggeshall, 1971).

Cytoskeletal elements are responsible for localization of channels to the plasma membrane (Levina et al., 1994; Smith et al., 1995; Huang et al., 2002; Schubert and Akopian, 2004). In BCNs, activation of PKC causes its translocation to the plasma membrane where it binds actin (Nakhost et al., 1998), suggesting that cytoskeletal dynamics play a role in downstream actions of PKC. We now show that, after PKC activation, the Ca_V2 channel, which resides within the central region of the growth cone in resting neurons, is transferred from microtubules to actin inside the lamellipodium at the distal growth cone edge, and then inserted at this location into the plasma membrane. The insertion of the Ca_V2 channel is dependent on the function of actin monomers. These events are part of the transformation of growth cones into mature neurosecretory endings (Knox et al., 1992).

Received Jan. 19, 2007; revised Jan. 24, 2008; accepted Jan. 24, 2008.

This work was supported by National Institutes of Health Grants NS 18492 (L.K.K.) and NS 45876 (E.A.J.). We thank Drs. Paul Forscher and Nurul Kabir for discussions in the early stages of this work.

Correspondence should be addressed to Elizabeth A. Jonas, Department of Internal Medicine, Section of Endocrinology, Yale School of Medicine, 333 Cedar Street, New Haven, CT 06520. E-mail: elizabeth.jonas@yale.edu.

DOI:10.1523/JNEUROSCI.4314-07

 0270-6474/08/282601-12$15.00/0

Materials and Methods

Animals and cell culture. Adult *Californica* weighing 100–200 g were obtained from Marine Specimens Unlimited (San Francisco, CA) or Marinus (Long Beach, CA). Animals were housed in a ~400 L aquarium containing continuously circulating, aerated Instant Ocean (Aquarium Systems, Mentor, OH) salt water at 14°C on an ~12 h light/dark cycle and were fed romaine lettuce three times a week. All experiments were performed at room temperature (18–20°C). For primary cultures of isolated bag cell neurons, animals were anesthetized by an injection of isotonic $MgCl_2$ (~50% of body weight); the abdominal ganglion was removed and treated with neutral protease for 18 h at 18–20°C (13.33 mg/ml; Boehringer Mannheim, Indianapolis, IN) and dissolved in normal artificial seawater (nASW); the nASW was composed of (in mM) 460 NaCl, 10.4 KCl, 11 $CaCl_2$, 55 $MgCl_2$, 15 HEPES, 1 mg/ml glucose, 100 U/ml penicillin, and 0.1 mg/ml streptomycin, with pH adjusted to 7.8 with NaOH. The ganglion was then transferred to fresh nASW, and the bag cell neuron clusters were dissected from their surrounding connective tissue. Using a fire-polished Pasteur pipette and gentle trituration, neurons were dispersed in nASW onto 35 × 10 mm polystyrene tissue culture dishes (Corning, Corning, NY). Cultures were maintained in nASW for 1–3 d in a 14°C incubator.

Electrophysiology. To measure the voltage-dependent Ca^{2+} current, isolated bag cell neurons were bathed in isomotic-substituted ASW, in which NaCl and KCl were replaced with 460 mM tetraethylammonium chloride (TEA-Cl) and 10.4 mM CsCl. Ba^{2+}currents were recorded by substituting $BaCl_2$ for $CaCl_2$. Inward currents can be studied in relative isolation using this solution (Kaczmarek and Strumwasser, 1984). The pipette solution was 3 M KCl, the pipette resistance was 3–10 MΩ. The membrane potential was held at −55 mV and then depolarized to potentials between −25 and +25 or +35 mV (300 ms pulses; 5 s interpulse intervals). Data were acquired with an Axoclamp 2A (single-electrode voltage-clamp mode) amplifier. Data were digitized, stored, and analyzed using Clampex 8.1 (pClamp). Current measurements were made at peak inward current.

Biotinylation of surface Ca_V2 and Ca_V1 proteins. Surface protein was detected using previously described methods (Ennion and Evans, 2002) with slight modifications. Intact clusters of bag cell neurons from adult *Aplysia* (150–250 g) were incubated for 18 h at room temperature in nASW containing 1% dispase. Experimental clusters were treated with 100 nM 12-*O*-tetradecancyl-phorbol-13-acetate (TPA; for 30 min, whereas untreated contralateral clusters from the same animals served as controls. Clusters were incubated with Sulfo-NHS-LC-Biotin (1 mg/ml; Pierce, Rockford, IL) in nASW for 30 min at room temperature. After washing, clusters were homogenized at 4°C in lysis buffer and centrifuged (16,000 × *g* for 2 min). Streptavidin agarose beads (50 μl, Pierce) were added to the supernatant which was shaken overnight at 4°C. After repeated washing, 40 μl of sample buffer containing 100 mM DTT was added and the beads rotated at 20°C for 2 h to cleave the beads from channel protein. After centrifuging at 16,000 × *g* for 2 min, 45 μl of the supernatant was separated by SDS-PAGE. Protein concentrations were assayed using a Bio-Rad (Hercules, CA) protein assay and equal amounts of proteins were added to each lane. Precision Plus protein Standards (Bio-Rad) were used as the protein molecular weight markers. Proteins were transferred from the gels to polyvinylidene difluoride (PVDF) membranes, and then probed with rabbit anti-*Aplysia* Ca_V2 calcium channel (1:200) or rabbit anti-*Aplysia* Ca_V1 calcium channel antibodies (1:200). The secondary antibody was donkey anti-rabbit Ig, horseradish peroxidase-linked whole antibody (1:5000; GE Healthcare Bio-Sciences, Piscataway, NJ). Labeled proteins were visualized by enhanced chemiluminescence (GE Healthcare Bio-Sciences).

Antibody production and purification. A peptide was synthesized to generate antibody against the cloned partial calcium channel sequence (White and Kaczmarek, 1997). This peptide (CXSEHYNQPEWFVD-FLYITE) included 18 aa near the N-terminal extracellular domain between membrane spanning regions S1 and S2 of domain I (see Fig. 2*A*). This sequence is 75% identical to that of the mammalian $Ca_V2.1$ channel. The peptide was synthesized at the W. M. Keck Biotechnology Resource Center, Yale University (New Haven, CT). The X in the sequence represents aminocaproic acid, which acted as a spacer molecule between the specific sequence and a nonspecific N-terminal cysteine, which allowed conjugation of peptides to the keyhole limpet hemocyanin (KLH) peptide. KLH, in turn, acted as a carrier for antigenic peptide in the generation of chicken polyclonal IgY, which was performed by Aves Labs (Tigard, OR). Antibody was precipitated using saturated ammonium sulfate. Antibody specificity with respect to preimmune IgY was verified with an enzyme-linked immunoabsorbent assay using the antigenic peptide, and antibody binding could be blocked by preabsorption with excess antigen.

Immunoprecipitation. Bag cell neuron clusters were dissected from 200 to 250 g animals in high-Mg^{2+} dissecting seawater (Eisenstadt et al., 1973). The clusters were pooled in groups of three and placed in 35 mm dishes containing nASW. Three groups of clusters were used to test whether Ca_V2 and tubulin coassociate before and after activation of PKC by treatment with TPA (100 nM) (Sigma, Oakville, Ontario, Canada), or TPA in the presence of 1 μM bisinodolylmaleimide (BIS; Sigma), an inhibitor of PKC. Three additional groups of clusters were used to test the association between Ca_V2 and actin: One group served as the control, the second group was treated with TPA (100 nM), and the third group was pretreated with BIS, before adding TPA. The clusters were then incubated for 30 min at room temperature. The clusters were homogenized in 400 μl of buffer (1% Lubrol, 50 mM Tris-HCl, pH 7.4, 10 nM Na-orthovanadate, 30 mM Na-pyrophosphate, 50 mM NaF, 20 μM $ZnCl_2$, and 0.25 mM PMSF, containing protease inhibitor mixture; Roche) in glass-glass tissue grinders for 3 min on ice. Samples were then centrifuged at 100,000 × *g* for 30 min. The supernatants were collected and transferred to 1.5 ml Eppendorf (Hamburg, Germany) tubes. Tubes were incubated at 4°C with rotation overnight after addition of 1 μg of purified intracellular anti-Ca_V2 calcium channel antibody (White and Kaczmarek, 1997) or addition of anti-IgG (either anti-rabbit for tubulin or anti-mouse for actin; The Jackson Laboratory, Bar Harbor, ME). After adding 30 μl protein A-Sepharose beads [50% (v/v) in Triton X-100 buffer; Sigma] the samples were rotated at 4°C for 2 h, and the immunoprecipitates were collected by centrifugation at 3000 × *g* for 1 min and washed twice in 800 μl of Triton X-100 buffer. The samples were applied to SDS-acrylamide gels. For the immunoblotting, the SDS gel-electrophoresed proteins were transferred to immunoblot PVDF membrane (Bio-Rad). Nonspecific binding was blocked by incubating the blot in Tris-buffered saline with Tween 20 (TBST) buffer with 5% milk for 1 h at room temperature. Blots were incubated with anti-tubulin antibody (1:500) developed in mouse (Sigma) or anti-actin antibody (1:400) developed in mouse for total protein lanes 1–3 and Ca_V2 IP lanes 1–3 (see Fig. 8*B*, right) or anti-actin developed in rabbit (1:200) for total protein (labeled total and IgG IP) (see Fig. 8*B*, left) (Sigma) overnight at 4°C, then washed four times for 30 min each, followed by application of secondary antibodies [horseradish peroxidase linked anti-mouse Ig (GE Healthcare Bio-Sciences) at 1:5000 dilution or anti-rabbit IgG (GE Healthcare Bio-Sciences) at 1:10,000 dilution for 1 h at room temperature]. After three washes of 30 min each in TBST, immunoreactive proteins were visualized with detection reagent (GE Healthcare Bio-Sciences).

Immunocytochemistry. Staining of cultured bag cell neurons was performed on coverslips coated with 1 μg/ml poly-D-lysine (Sigma). Bag cell neurons were cultured in nASW for 1–2 d before fixation with 4% paraformaldehyde in 400 mM sucrose/nASW, as described previously (White and Kaczmarek, 1997). Three milliliters of fixative solution were then rapidly superfused into the central well, and fixation was allowed to continue for 25 min before the addition of Triton X-100 (0.3%). In experiments using the antibody to the extracellular epitope, the permeabilization step was omitted. Nonpermeabilized cells were not immunoreactive with an anti-tubulin antibody that only binds to an intracellular epitope ($n = 2$) (see Fig. 4*E*). Culture dishes were then washed twice with PBS and blocked with 5% goat serum/PBS before incubation with primary antibodies. Coverslips were removed from the culture dishes, inverted on 100 μl of primary antibody solution, and placed in a humidified chamber at 4°C overnight. The primary antibody concentration was used as 1:200 intracellular Ca_V2 calcium channel antibody in 5% goat serum/PBS or extracellular Ca_V2 calcium channel antibody, 1:100. For experiments with Na^+-K^+ ATPase β2, antibody was used at 1:500 (BD

Biosciences, Franklin Lakes, NJ). After overnight incubation, the coverslips were washed extensively with PBS and then incubated for 2 h at room temperature with fluorescein or Cy3-conjugated goat anti-rabbit IgG secondary antibodies (FITC-GαRigG or Cy3-GαRigG, respectively; Invitrogen, Carlsbad, CA), or fluorescein-conjugated goat anti-chicken IgG secondary antibodies (FITC-GaCigG; Invitrogen). For Na^+-K^+ ATPase $\beta 2$, secondary antibody was FITC-conjugated anti-mouse IgG (Invitrogen). Coverslips were washed and mounted on glass slides using mounting medium. The stained slides were viewed and photographed using standard epifluorescence and differential interference contrast or phase optics using an Axiovert 200 microscope and Axiovision software (Zeiss, Oberkochen, Germany). All fluorescent images of the antibody to the extracellular domain were made with the same exposure time. Measurements of fluorescence were made by converting the Axiovision files to TIFF files. Regions of interest (ROIs) were defined (4–25 μm^2) using Adobe (San Jose, CA) Photoshop 7.0 and the average pixel intensity for each ROI was calculated. Background intensity measured from an area of the image devoid of cells was subtracted from each measurement. An area of maximum fluorescence in each part of the cell under study was used to create the ROI. In ROIs made of the distal growth cone, an area of maximum fluorescence just at the edge of the lamellipodium was used to create the ROI. To compare the fluorescence near the edge of the lamellipodium to that of the central region of the growth cone in Figure 5 a ratio was made of the intensity of fluorescence of the ROIs from the two sites. Raw data were used for all measurements.

GripTite 293 macrophage scavenger receptor (MSR) cells were cultured as indicated by the manufacturer (Invitrogen) and supplemented with 1% (v/v) penicillin–streptomycin antibiotic solution (Sigma). Cells were transfected using the calcium phosphate method with 6.7 μg of either *Lymnaea stagnalis* LCa_V1 channel (Spafford et al., 2006) or LCa_V2 channel (Spafford et al., 2003) α_1 subunits in phosphorylated internal ribosomal entry site-enhanced green fluorescent protein (pIRES2-EGFP) vector (Clontech Laboratories, Mountain View, CA) plus 6.7 μg of rat β_1 subunit in pMT2 and 6.7 μg of rat $\alpha_2\delta$ in pMT2. Transfected cells were subsequently washed with PBS and detached using trypsin-EDTA solution (Sigma). Transfected cells were combined 1:1 with untransfected cells and these preparations were incubated at 28°C for 5 d in culture dishes containing coverslips coated with 0.1 mg/ml poly-L-lysine (Sigma). After incubation cells were washed twice with warm PBS and fixed with 1% paraformaldehyde in PBS preheated to 37°C at room temperature for 2 h then 4°C overnight. After fixation cells were washed twice with PBS then once with PBS and 0.2% Tween 20 (PBS-T) and once with PBS-T containing 1% BSA (PBS-T 1% BSA). Cells were then blocked with PBS-T 3% BSA and incubated at room temperature for 2 h. Saturated ammonium sulfate-precipitated chicken anti-*Aplysia* Ca_V2 antibodies were diluted 1:200 in PBS-T 3% BSA and cells were incubated with primary antibody solution overnight at 4°C. For controls lacking primary antibody, coverslips were incubated in PBS-T 3% BSA lacking antibody. Cells were washed three times, 20 min per wash, with PBS-T 3% BSA then blocked with PBS-T 5% BSA for 45 min. Cells were then incubated for 45 min at room temperature with Alexa Fluor 633 goat anti-chicken IgG (heavy and light) (Invitrogen) secondary antibody diluted 1:5000 in PBS-T 3% BSA, then washed three times with PBS-T and 1 × with PBS. Coverslips were dried at 37°C for 30 min and mounted onto glass slides using FluorSave Reagent (Calbiochem, La Jolla, CA and EMD Chemicals, San Diego, CA). Images were captured using a Zeiss LSM 510 META confocal microscope and Argon/HeNe lasers to excite samples at 488 and 633 nm, respectively. Detection was performed between 505 and 530 nm for EGFP and >650 nm for the Alexa Fluor 633 dye. Zeiss LSM 510 META software was used to acquire and adjust the brightness and contrast of all images.

Live cell imaging. The rabbit Ca_V2 calcium channel antibody was conjugated with fluorescent probe Alexa Fluor 594 according to the manufacturer's instructions (Invitrogen). Briefly, calcium channel antibody (2 mg/ml) was mixed with a succinimidyl ester moiety of Alexa Fluor 594 for 1 h at room temperature to form a stable dye-protein combination. The labeled protein was purified by using column chromatography provided with the kit, resulting in separation of the conjugated protein from the free dye. Cultured bag cell neurons were incubated with 250 nM Tubulin Tracker (Invitrogen) for 30 min and then thoroughly washed. Pressure injections of the fluorescence-labeled calcium antibody were made into the tubulin-labeled cells (typically 1–10 pulses; 100 ms, 5 psi) using a Picospritzer (General Valve, Fairfield, NJ). Injection solutions contained 11 mM Tris-Cl, pH 7.2, 530 mM potassium acetate. Control cells were injected with secondary anti-rabbit Cy3 (594 nm) in injection solution. Images of injected cells were captured using a Zeiss Axiovert microscope equipped with an Argon/HeNe laser.

Actin staining. For fluorescent staining of the actin cytoskeleton, cells were fixed on glass coverslips with 4% freshly made paraformaldehyde in isotonic ASW supplemented with 400 mM sucrose, pH 7.8 (Lin and Forscher, 1993). After fixation, cells were permeabilized for 10 min in fixation buffer plus 1% Triton X-100, washed with PBS, and stained with Alexa Fluor 488-conjugated phalloidin (Invitrogen) in PBS. Cells were then washed with PBS, exposed to 5% goat serum albumin-PBS, followed by purified rabbit intracellular antibody anti-calcium channel, washed with PBS, exposed to Cy3 conjugated goat anti-rabbit secondary antibody (Invitrogen), then washed with PBS. One drop of AquaMount was placed on each glass slide before applying a coverslip.

Results

Enhanced calcium current results from insertion of Ca_V2 channels into the plasma membrane

Previous data has shown that the PKC activator TPA increases calcium currents and enhances the calcium component of action potentials in BCNs (DeRiemer et al., 1985). These actions of TPA are mimicked by the structurally unrelated diacylglycerol activators of PKC and by direct microinjection of this enzyme, and can be prevented by PKC inhibitors including pseudosubstrate peptide inhibitors (Conn and Kaczmarek, 1989; Conn et al., 1989a,b). Cell-attached patch recordings at the soma also demonstrate that, in response to activation of PKC, a new species of calcium channel that has a different conductance from that observed in untreated neurons can be detected (Strong et al., 1987). Confirming previous work, we found, using single-electrode voltage-clamp recording, that treatment of cells with TPA caused an approximately twofold increase in peak amplitude of calcium currents elicited by a series of depolarizing pulses (Fig. 1*A*) (from 1.11 ± 0.1 nA to 1.98 ± 0.2 nA; $p < 0.0001$; $n = 19$). These electrophysiological results confirmed that the calcium current, which likely reflects channel activity at the soma and proximal neurites, was modulated by PKC, but did not address whether channel was being inserted into the membrane during the process of current enhancement. We therefore tested whether new calcium channels could be detected in the plasma membrane after TPA treatment using biotinylation of surface Ca^{2+} channel subunits and by immunocytochemical techniques.

In BCNs, two species of calcium channel can be differentiated by specific antibodies. Ca_V2 localizes to intracellular organelles and is enriched in the central region of the growth cone (Nick et al., 1996; White and Kaczmarek, 1997). The other α-subunit, Ca_V1, which appears to be responsible for the calcium current that can be recorded in the absence of PKC activation, is localized predominantly to the soma plasma membrane by immunocytochemistry and very little intracellular staining for Ca_V1 is detected (White and Kaczmarek, 1997). Surface biotinylation of proteins in clusters of intact bag cell neurons was used to detect levels of these two channel subunits in the presence and absence of TPA (Fig. 1*B*). Little Ca_V2 immunoreactivity could be detected in the surface proteins of control untreated clusters. In contrast, treatment with TPA for 30 min produced a marked increase in levels of the Ca_V2 subunit at the surface. Densitometric analysis indicated that levels of Ca_V2 at the plasma membrane increased more than threefold (Fig. 1*C*). When the preparations of surface pro-

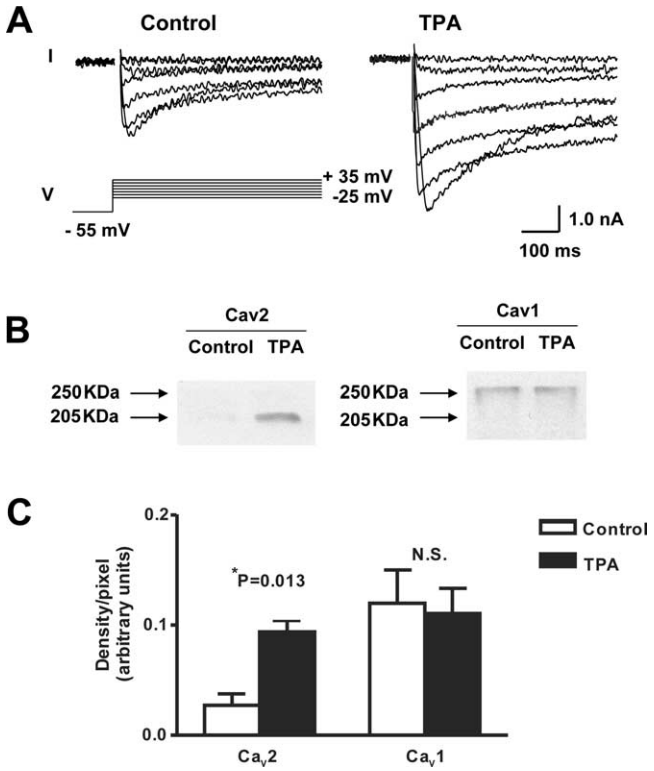

Figure 1. Activation of PKC enhances voltage-dependent calcium current and increases levels of Ca_V2 in the plasma membrane of bag cell neurons. ***A***, Single-electrode voltage-clamp records of inward current carried by barium ions through calcium channels in a bag cell neuron before and 10 min after exposure of the cells to 100 nM TPA (see Materials and Methods). The holding potential was −55 mV and the membrane potential was stepped to potentials between −25 and +35 mV in 10 mV increments. ***B***, Western blots showing levels of plasma membrane Ca_V2 subunit (left two lanes) or Ca_V1 subunits (right two lanes) in clusters of bag cells neurons in the presence or absence of the PKC activator TPA (100 nM for 30 min). Antibodies used were to intracellular epitopes on the Ca_V2 and Ca_V1 channels (White and Kaczmarek, 1997). Plasma membrane subunits were detected on Western blots after biotinylation of cell surface proteins followed by separation of biotinylated proteins using streptavidin agarose beads. Results are representative of 3 independent experiments. ***C***, Quantification of the effect of TPA on cell surface expression of Ca_V2 using densitometric analysis.

teins were probed with antibody for Ca_V1, no change in surface expression was detected after TPA treatment (Fig. 1*B*,*C*).

To confirm further that the intracellular Ca_V2 channel is inserted into the plasma membrane after activation of PKC, and to locate sites of insertion, we generated an antibody against an extracellular epitope between membrane spanning regions S1 and S2 in domain II of the *Aplysia* Ca_V2 channel (Fig. 2*A*) (White and Kaczmarek, 1997). On Western blots of homogenates of bag cell neurons, this antibody recognized a band of 205 kDa, the appropriate size for the Ca_V2 channel (Fig. 2*B*). As a further test for specificity of this antibody, we transfected mammalian GripTite 293 MSR cells with the *Lymnaea* Ca_V2 channel (Spafford et al., 2003; Spafford et al., 2004), which differs from the *Aplysia* Ca_V2 channel in only 2 of the 18 aa of the sequence against which the antibody was generated [SEHYNQPEWHVQFLYITE (*Lymnaea*) vs SEHYNQPEWFVDFLYITE (*Aplysia*)]. Cells were also transfected with the full-length *Lymnaea* Ca_V1 channel (Spafford et al., 2006). These channels were expressed in the pIRES2 bicistronic vector, where EGFP is coupled to the mRNA of LCa_V2 and LCa_V1, allowing ready visualization of transfected cells. Immunoreactivity to the extracellular epitope of Ca_V2 was selectively observed in LCa_V2 expressing cells that were either nonpermeabilized (Fig. 2*C*, top row) ($n = 2$ experiments) or permeablized ($n = 6$) (data not shown) but was absent in LCa_V1 expressing cells (Fig. 2*C*, bottom row). No staining was observed in LCa_V2 transfected cells in the absence of primary antibodies (Fig. 2*C*, center row).

We used the antibody to the extracellular epitope to localize Ca_V2 channels only as they appeared on the surface of the plasma membrane in nonpermeabilized BCNs. Exposure to an activator of PKC for short periods of time (5–30 min) expands the distal edge of the lamellipodium but does not increase the number of neuritic branches (Knox et al., 1992). Activation of PKC by TPA caused an enhancement of intensity, and an alteration in distribution, of plasma membrane Ca_V2 immunofluorescence in treated cells compared with control, untreated cells (Fig. 2*D*,*E*). At low magnification, after activation of PKC, fluorescence intensity was increased in the soma and in the neurites, highlighting distal regions of the cell that were present but had not been stained in control cells (Fig. 2*D*). At increased magnification, where only the neurites were imaged, fluorescence could be seen in the most distal growth cone edge with much greater frequency in TPA treated cells compared with controls (Fig. 2*E*). Measurements were made of the intensity of the fluorescence in control and TPA treated cells prepared from the same bag cell clusters. The average pixel intensity of fluorescence at the distal tips of the growth cones in control cells was 0.76 ± 0.29 ($n = 8$), whereas that in TPA treated cells was 7.76 ± 1.2 ($n = 17$, $p < 0.0005$) (see Fig. 4*F*). These findings confirmed the appearance of new immunoreative Ca_V2 channels in the distal edge of the lamellipodium.

Latrunculin B prevents the PKC-induced increase in calcium current

The cytoskeleton regulates the insulin-dependent translocation of the glucose transporter to the membrane (Tong et al., 2001). In addition, cytoskeletal motors regulate ion channel function (Furuyashiki et al., 2002) and exocytosis in neurons (Muallem et al., 1995; Lang et al., 2000). Cytoskeletal dynamics could therefore play a role in targeting the calcium channel to sites of insertion.

To test whether polymerized actin is necessary for channel insertion, we used inhibitors of actin that work in different ways while treating with TPA. Latrunculin B sequesters actin monomers, preventing the formation of new polymerized actin (Brozinick et al., 2004). Treatment of bag cell neurons with latrunculin B alone did not produce a statistically significant increase in calcium current (control, 1.38 ± 0.23 nA; latrunculin B, 1.25 ± 0.21 nA; $n = 8$). Pretreatment with latrunculin B (10 μM) for 1 h effectively prevented the increase in calcium current produced by TPA (Fig. 3*A*) (from 1.53 ± 0.38 nA to 1.49 ± 0.36 nA; $n = 8$). Cytochalasins are a group of fungal metabolites that act differently from latrunculin B. They selectively disrupt actin filaments by binding to these filaments at their plus and minus ends and preventing filament elongation (Morton et al., 2000). They thereby eventually cause depolymerization of actin as observed by confocal laser scanning of neurons stained with a fluorescently labeled phalloidin that binds to polymerized actin (Cooper, 1987). Pretreatment of the bag cell neurons with cytochalasin B for 30 min did not prevent the increase in calcium current produced by application of TPA (from 1.15 ± 0.05 nA to 2.34 ± 0.08 nA; $n = 4$; $p < 0.0001$) (Fig. 3*B*). Together, these results indicate that the increase of calcium currents produced by TPA, which, as stated previously, is likely to reflect channel activity at the soma and proximal neurites, is dependent on actin, but suggest that polymerization of actin monomers is necessary for the effects of TPA (Morton et al., 2000).

Because PKC has been shown to modulate microtubule exten-

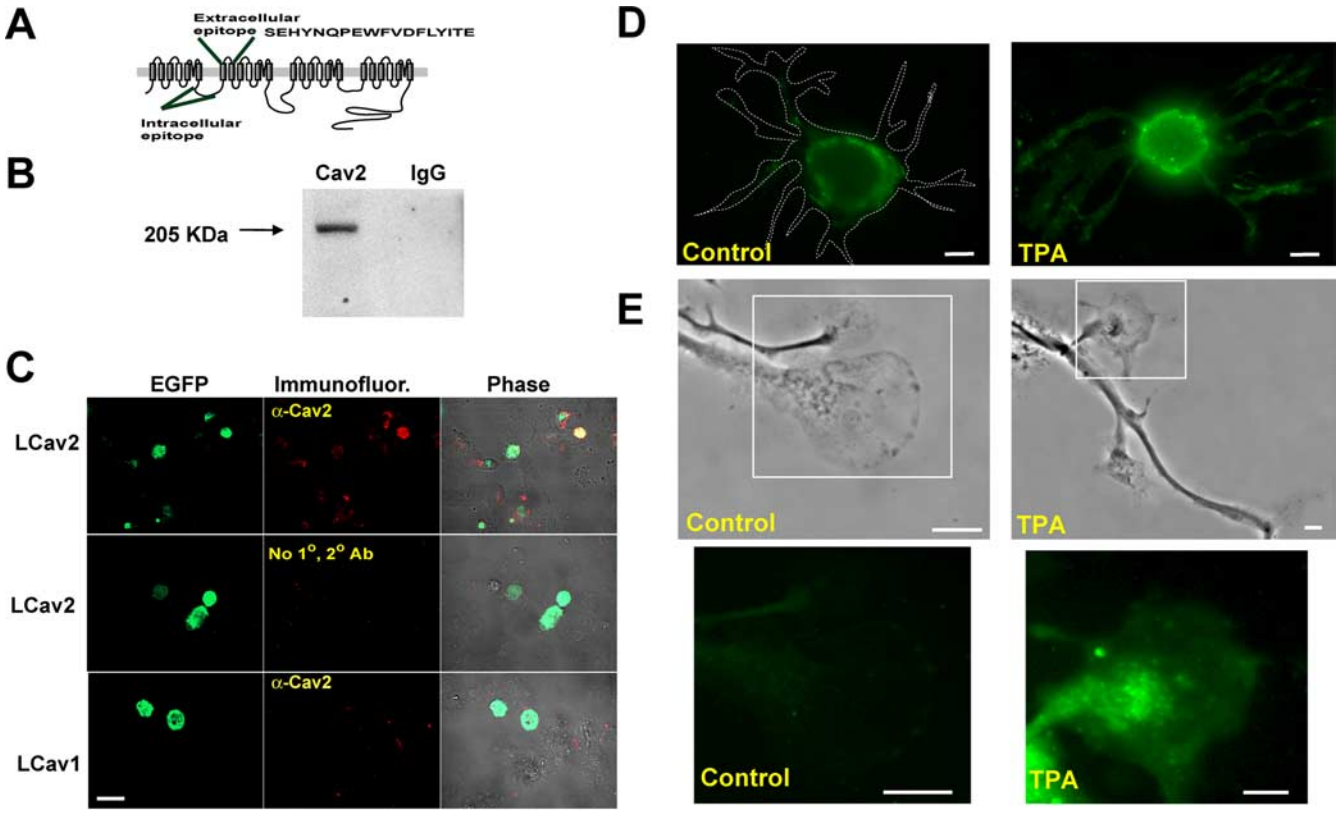

Figure 2. Activation of PKC results in enhanced Ca_V2 immunoreactivity in the plasma membrane of bag cell neurons. ***A***, Diagram showing location of epitopes against which antisera were generated for the *Aplysia* Ca_V2 calcium channel. ***B***, Western blot of homogenate of bag cell neurons probed with the anti-Ca_V2 antibody targeted to the extracellular epitope. ***C***, Immunostaining of nonpermeabilized GripTite 293 MSR cells transfected with *Lymnaea stagnalis* Ca_V2 channels using chicken anti-*Aplysia* Ca_V2 channel antibody targeted to extracellular epitope. Top row, Cells transfected with *L*Ca_V2 in pIRES2-EGFP showing EGFP fluorescence (left) and colocalization of *L*Ca_V2 immunofluorescence (middle). Middle row, Cells similar to those in the first row lacking primary antibody showing EGFP fluorescence but no *L*Ca_V2 immunofluorescence. Bottom row, Cells transfected with *L*Ca_V1 in pIRES2-EGFP showing EGFP fluorescence but no immunofluorescence. Results are representative of eight independent experiments. Scale bar, 20 μm. ***D***, Immunocytochemical localization of Ca_V2 channels in nonpermeabilized cells using an antibody to the extracellular epitope. Cells plated from the same clusters were either incubated in nASW (left) or exposed to 100 nM TPA (right) for 30 min before fixing. The dotted line in the control indicates neurites that were unstained or only faintly stained with antibody. Scale bars, 20 μm. ***E***, Phase images of axons and growth cones of a control and TPA-treated cell. Fluorescent images corresponding to the areas of detail (white boxes) are expanded below the phase images, and show immunolocalization of the α-Ca_V2 extracellular epitope in the absence of membrane permeabilization. Scale bars, 10 μm.

sion (Keenan and Kelleher, 1998), and because microtubules play an important role in vesicle trafficking (Huang et al., 1999; Prahlad et al., 2000; Gauthier et al., 2004; Yano and Chao, 2004), we investigated whether microtubules are required for calcium channel translocation into the plasma membrane during PKC activation. We first tested the effects of nocodazole and taxol, two agents that disrupt normal microtubule dynamics, on calcium currents. These agents did not alter the peak amplitude or kinetics of calcium currents in control bag cell neurons before treatment with TPA. After exposure to either taxol or nocodazole, treatment with TPA caused a large increase in calcium current peak amplitude that could not be distinguished from the response of control cells (with taxol, currents increased from 0.87 ± 0.12 nA to 1.9 ± 0.2 nA, $p < 0.005$, $n = 4$; with nocodazole, currents increased from 1.1 ± 0.07 nA to 2.18 ± 0.2 nA, $p < 0.002$, $n = 4$) (Fig. 3*B*). The findings suggested that microtubules are not necessary for the increase in current produced by activation of PKC.

The electrophysiological findings showed that the calcium current of the cell as a whole was increased in response to TPA. The studies with the antibody to the extracellular epitope suggested that activation of PKC resulted in channel insertion in certain parts of the cell, including the soma, but also, in particular, at the distal growth cone edge (the lamellipodium), which is relatively devoid of microtubules and contains different forms of actin (Knox et al., 1992; Nakhost et al., 2002). To arrive at this distal edge, however, vesicles containing Ca_V2 channels may move down the axon by transport along microtubules (Huang et al., 1999; Prahlad et al., 2000; Gauthier et al., 2004; Yano and Chao, 2004), or the channel may be inserted into the membrane and then moved within the membrane toward the growth cone edge. Using the antibody directed against the extracellular epitope, the increase in immunoreactivity of Ca_V2 could be seen clearly in the central region of the growth cone and in the tips of neurites after activation of PKC (Fig. 4*A*,*B*,*F*). To determine whether the effect of TPA on Ca_V2 immunoreactivity is specific to these channels or results from the general insertion of membrane associated with an increase in the lamellipodia, we also quantified immunoreactivity of the plasma membrane marker Na^+-K^+ ATPase at the distal tips of lamellipodia in nonpermeabilized control and TPA treated cells (Fig. 4*G*). The intensity of immunofluorescence measured at the distal edge of the stained growth cones was performed as in Figure 4*F*. No significant difference in Na^+-K^+ ATPase staining was detected between the two conditions [controls, 45 ± 6.7 relative fluorescence units (rfus), $n = 10$; TPA-treated cells, 43 ± 4.3 rfus, $n = 7$].

Consistent with the findings for voltage-clamp recordings, treatment with latrunculin B effectively prevented the appearance of Ca_V2 channel immunoreactivity in response to TPA anywhere in the plasma membrane (Fig. 4*C*,*F*). In contrast to treat-

ment with latrunculin B, however, treatment with nocodazole and TPA caused a significant increase in fluorescence of the neurite shaft and the central growth cone compared with controls. Strikingly, however, this fluorescence was excluded from the distal growth cone edge (Fig. 4*D*,*F*). Although the increases in fluorescence at the shaft and the central growth cone were slightly larger than those observed with TPA alone, these differences were not statistically significant. These findings are also consistent with the electrophysiological data, which show TPA enhances calcium current in the presence of nocodazole. Although channel insertion in response to activation of PKC occurs in the presence of nocodazole, the inserted channels appear to be mislocalized, failing to insert at the distal growth cone edge.

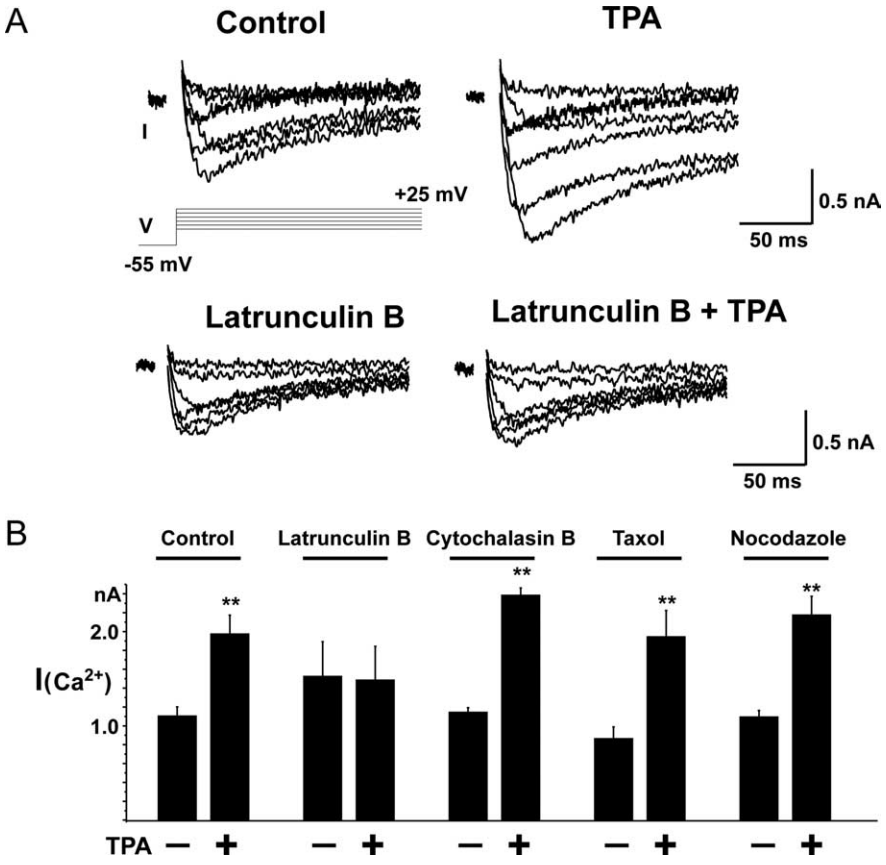

Figure 3. Enhancement of calcium current by TPA is blocked by latrunculin B but not by cytochalasin B, taxol, or nocodazole. ***A***, Single-electrode voltage-clamp recordings of barium current in a control neuron before and 10 min after exposure to 100 nM TPA and in one pretreated with latrunculin B (10 μM for 60 min). The holding potential was −55 mV and the membrane potential was stepped to potentials between −25 and +25 mV in 10 mV increments. ***B***, Bar graphs showing the peak calcium current at 0 mV before and after exposure to 100 nM TPA in control cells ($n = 19$) and in those pretreated for 60 min with latrunculin B (10 μM, $n = 8$), cytochalasin B (7 μM, $n = 4$), taxol (1 μM, $n = 4$), or nocodazole (100 nM, $n = 4$). Data are expressed as mean ± SEM. **Significant difference from control at $p < 0.001$.

Calcium channel moves to the lamellipodium after activation of PKC

The cytoskeleton of the growth cone can be organized into central and peripheral domains. A large bundle of microtubules predominates in the central domain (C) and a subpopulation of dynamic microtubule plus ends penetrates into the peripheral lamellipodial domain (L), where actin bundles comprise the radial array of filopodia and a dense actin meshwork spans the space between filopodia (Kabir et al., 2001). To test the hypothesis that PKC induces movement of intracellular channels into the peripheral actin-rich lamellipodium before insertion into the plasma membrane, we examined the location of Ca_V2 channels before and after activation of PKC, using an antibody to the intracellular epitope (Fig. 2) (White and Kaczmarek, 1997; White et al., 1998). The distribution of Ca_V2 was compared with that of the actin probe phalloidin. Immunolabeling of controls revealed a punctate distribution of calcium channel staining along the inside of the neurite, and within the central region of the growth cone, but only a small amount of immunoreactivity was detected in the phalloidin-stained lamellipodium ($n = 23$; L zone) (Fig. 5*A*). In TPA treated neurons, however, intracellular channel immunoreactivity was markedly increased in this distal actin-rich region and was colocalized there with fluorescent phalloidin ($n = 41$) (Fig. 5*B*). The ratio of Ca_V2 fluorescence (pixel intensity) in the distal tip of the growth cone to that in the central region of the growth cone in untreated neurites was found to be 0.32 ± 0.06. The ratio of Ca_V2 channel staining in the distal tip of the growth cone to the central region of the growth cone in neurons treated with TPA was found to be 0.68 ± 0.10 ($p < 0.001$). After prolonged exposure to TPA (Fig. 5*B*, bottom), channel immunoreactivity at the tips of the growth cones became less punctate and more diffuse, consistent with channel insertion into the membrane. The results suggest that TPA causes the relocalization of the channel to the distal actin-rich sites.

Usually, after activation of PKC, puncta of calcium channel staining were seen arrayed along a straight actin filament or staining was diffusely distributed within the lamellipodium. In some examples, however, after activation of PKC, rows of immunoreactive puncta could be seen arranged in a snakelike manner within the distal tip of the lamellipodium, similar to that reported for "stealth" microtubules that invade the lamellipodial region (Kabir et al., 2001) (Fig. 5*C*). This finding suggested that after activation of PKC, during transfer to the actin-rich domain, channel could be colocalized with a microtubule within the lamellipodium (Nakhost et al., 2002).

To detect displacement of the Ca_V2 channel from the central region of the growth cone into the lamellipodial region, we fluorescently labeled both microtubules (green fluorescent tubulin tracker) and the antibody against the intracellular epitope of Ca_V2 (red fluorescence), and injected the labeled antibody into living, cultured bag cell neurons ($n = 6$). Before activation of PKC, fluorescent puncta could be observed colocalized with microtubules within the central region of the growth cone, but few fluorescent puncta were detected within the lamellipodial region (Fig. 6*A*,*B*). Some puncta appeared to be colocalized with discrete microtubule bundles labeled with tubulin tracker (Fig. 6*A*,*B*, insets). After activation of PKC, microtubules extended into the lamellipodial region and Ca_V2 fluorescent label could be detected in puncta distributed along the microtubule extensions (Fig. 6*A*,*B*, insets). As a control we performed experiments in which we injected a fluorescent secondary antibody. These injections did not produce any punctate labeling characteristic of

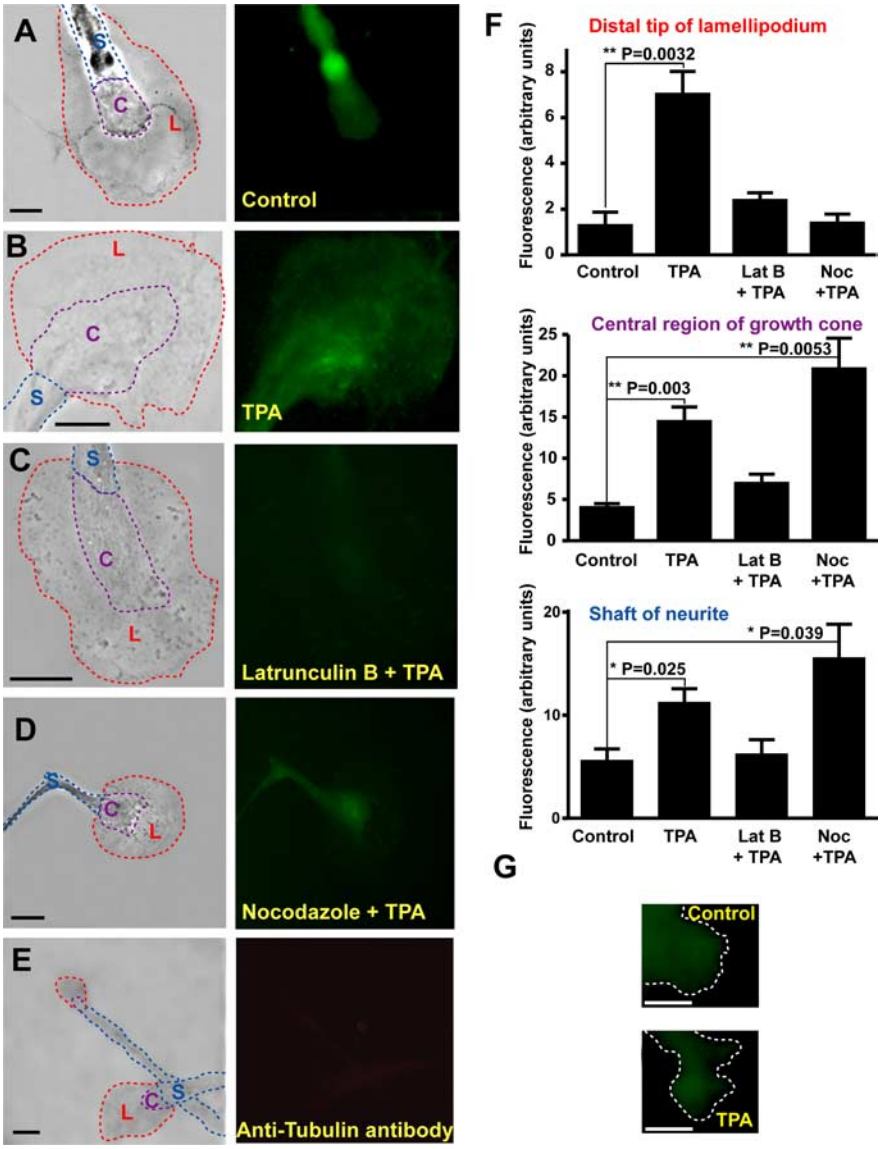

Figure 4. Translocation of Ca_V2 to the plasma membrane is blocked by latrunculin, but not by nocodazole. ***A–D***, Phase contrast (left) and immunostaining (right) of growth cones of nonpermeabilized cells with antibody to the extracellular epitope of Ca_V2. Dotted lines outline the shafts (S) of the neurites, the central organelle-rich region of the growth cone (C) and the flat lamellipodium (L) that is relatively devoid of organelles. Examples are shown of a control growth cone (***A***), one exposed to 100 nM TPA (***B***), one pretreated with latrunculin B (10 μM) before TPA application (***C***), and one pretreated with nocodazole (100 nM) before TPA application (***D***). ***E***, Phase contrast (left) and immunostaining of nonpermeabilized growth cones (right) with an antibody to an intracellular epitope (tubulin), showing that the cell has not been permeabilized by the procedure. Scale bars, 10 μm. ***F***, Bar graphs plot surface anti-Ca_V2 fluorescence of stained growth cones as the mean intensity per unit area at the distal edge of lamellipodia, in the central region of the growth cones and in the shaft of neurites, in the presence or absence of TPA with and without pretreatment with latrunculin B (10 μM) or nocodazole (100 nM). Data represent mean ± SE. For controls, $n = 5$; for TPA-treated, $n = 13$, for latrunculin B with TPA, $n = 12$, and for nocodazole with TPA, $n = 8$. ***G***, Immunostaining of growth cones for the plasma membrane marker Na^+-K^+ ATPase in control and TPA treated cells. The dotted lines in images outline the distal edge of the lamellipodia.

Ca_V2-containing organelles, but produced only diffuse staining that was unaffected by activation of PKC (Fig. 6*C*). The data suggest that the Ca_V2 channel is translocated into the distal lamellipodium along microtubule extensions.

To confirm that microtubules and not actin actually deposited channel inside the actin-rich lamellipodium, we tested whether latrunculin treatment could block the localization of intracellular channel to this zone in the presence of TPA. After activation of PKC, in the fixed cells, fluorescent labeling of the intracellular epitope of Ca_V2 could be detected at the very distal edge of the growth cone in either TPA ($n = 41$) or TPA/latrunculin-treated neurons ($n = 16$) (Fig. 7*A*,*C*,*D*), suggesting that actin polymerization is not required for the intracellular transport of the channel to the distal lamellipodium in response to activation of PKC. In contrast, nocodazole prevented the increase in fluorescence at the distal lamellipodial edge, confirming that intact microtubules are required for translocation through the lamellipodium up to the plasma membrane at the edge of the cell ($n = 18$) (Fig. 7*B*,*D*).

Binding of calcium channel to actin occurs in the actin-rich lamellipodium after activation of PKC

To test further whether the mechanism of calcium channel translocation involves transfer of the channel protein from microtubules to actin, we incubated clusters of bag cell neurons with and without TPA, and we then tested for coimmunoprecipitation of the Ca_V2 channel with actin or tubulin. In controls, tubulin could be coimmunoprecipitated by anti-Ca_V2 antibodies, but no actin was detected in the immunoprecipitate (Fig. 8*A*,*B*). After treatment with TPA, however, both actin and tubulin immunoreactivity were immunoprecipitated with the anti-Ca_V2 antibody (Fig. 8*A*,*B*). The coimmunoprecipitation of actin with Ca_V2 that was induced by TPA could be prevented by pretreatment of the cells with 1 μM BIS, an inhibitor of PKC before exposure of the intact cells to TPA (Fig. 8*A*,*B*,*C*), suggesting that activation of PKC results in the transfer of some channel protein between the two cytoskeletal proteins. Specificity of coimmunoprecipitation was tested using control IgGs (Fig. 8*A*,*B*). The control IgG and the Ca_V2 coimmunoprecipitations were performed in parallel using the same homogenates from the same animals, but were run on separate gels. Although immunoprecipitations are subject to many variables that can differ from blot to blot, the fact that there is a very strong actin immunoreactive band in total protein, but absolutely no signal whatsoever in the control IgG immunoprecipitates under any of the three experimental conditions (in the presence or absence of TPA), suggests that nonspecific Ca_V2-actin coimmunoprecipitation only under conditions of TPA treatment is highly unlikely. Additional control experiments in which protein was extracted from bag cell neuron clusters with and without TPA followed by Western blotting for Ca_V2 demonstrated that total Ca_V2 protein levels are not altered by TPA treatment (Fig. 8*D*).

Discussion

A PKC-induced increase in the calcium component of action potentials occurs at the onset of neuropeptide secretion in bag

cell neurons (Conn et al., 1989a). Our current findings have demonstrated directly that, after activation of PKC, Ca_V2 channels are rapidly inserted into the plasma membrane of BCNs from an internal pool of Ca_V2-containing granules. In resting neurons, before PKC activation, there was little biotinylation of cell surface Ca_V2 channels, which correlates well with the finding that the 24 pS PKC-regulated calcium channels cannot be detected by patch-clamp techniques before PKC activation (Strong et al., 1987). The weak Ca_V2 staining that could sometimes be detected at the soma in control cells may reflect either a basal level of PKC activation in these cells, or that a small fraction of Ca_V2 channels is resident in the membrane before PKC activation.

Enhancement of calcium current through the activation of PKC leads to new sites of calcium influx at two locations, the soma and the distal tips of growth cones (Knox et al., 1992). Because both the PKC-induced increase in macroscopic calcium current, which likely reflects primarily channel activity at the soma, and the appearance of surface Ca_V2 channels at growth cone terminals could be inhibited by latrunculin B, the findings suggest that a similar mechanism of channel recruitment, requiring actin polymerization from monomers, occurs at both locations.

Because the surface to volume ratio of terminals is much greater than that of somata, it is likely that channels at terminals represent a small fraction of the channels of the cell. Nevertheless, because neuropeptide secretion occurs in neurites, these channels within terminals play an important physiological function. Indeed, our current findings have demonstrated that, after activation of PKC there is a rapid trafficking of Ca_V2-containing organelles along microtubules into the distal actin-rich growth cone edge before insertion, possibly correlated with the onset of competence for neurosecretion.

Spatial and temporal regulation of actin rearrangements play roles in a wide array of cell functions (Watson et al., 2004). In BCNs, the neurites contain filamentous and globular actin, with tracks of microtubules. In contrast, the distal growth cone contains several forms of actin, and usually excludes microtubules (Nakhost et al., 2002), but "stealth" microtubules invade the actin-rich region after activation of PKC (Kabir et al., 2001). Our finding that tubulin can be coimmunoprecipitated with Ca_V2 subunits is likely to reflect the association of the Ca_V2 containing organelles with both axonal microtubules, as well as with the lamellipodial "stealth" microtubules, although, in such coimmunoprecipitation experiments we cannot exclude the possibility that the channel subunits bind monomeric tubulin. Nevertheless, our findings that the interaction of the cytoskeletal proteins actin and tubulin are required for trafficking and insertion into the plasma membrane of Ca_V2 subunits provide new roles for them in the rapid modulation of neuronal excitability.

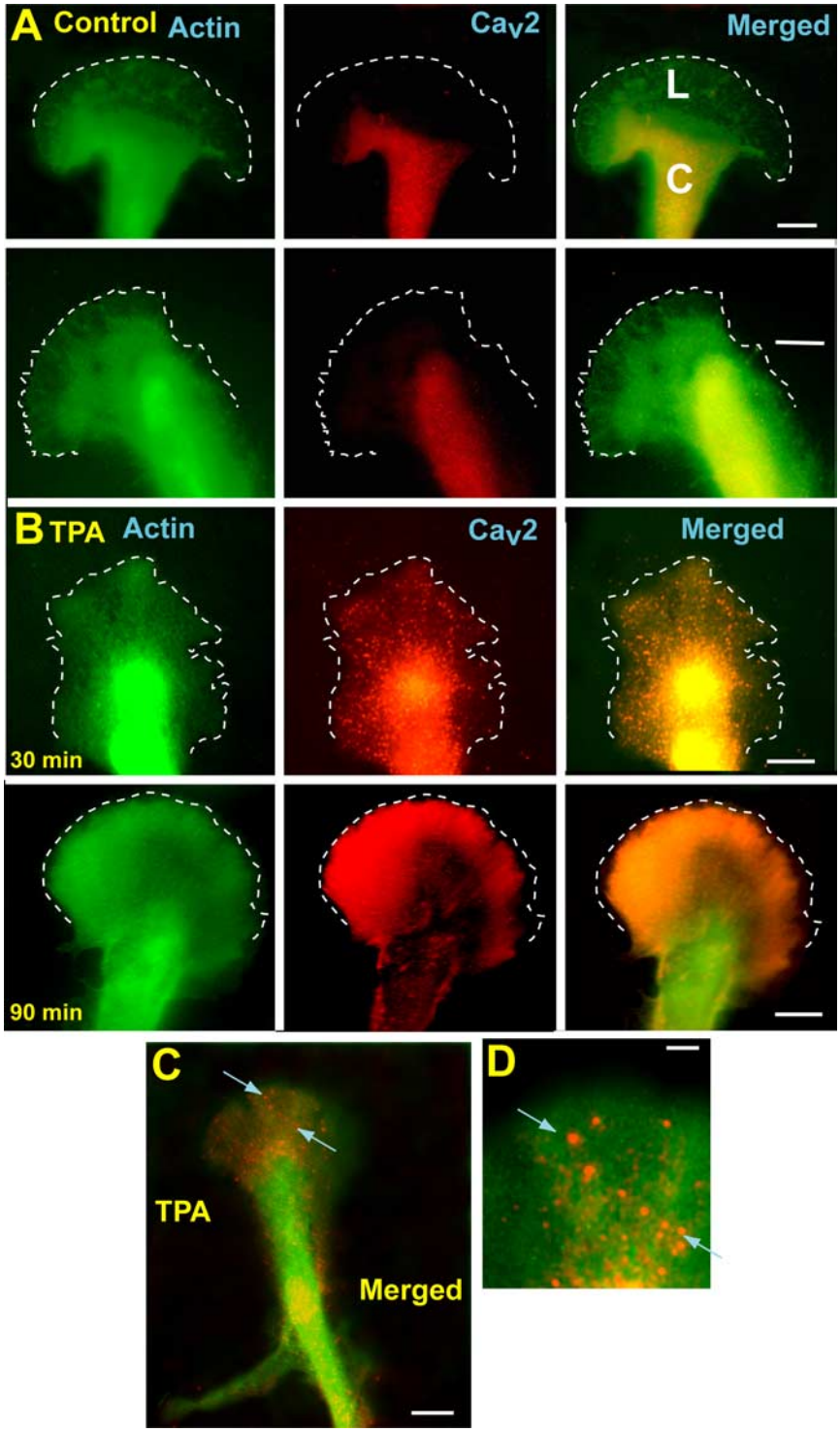

Figure 5. Calcium channels colocalize with actin in the lamellipodia of bag cell neurons after activation of PKC. Ca_V2 subunits were localized using an antibody to an intracellular epitope in permeabilized cells. ***A***, ***B***, Panels show staining for actin, Ca_V2, and the superimposed pattern of staining for two representative control untreated growth cones (***A***) and for two treated with 100 nM TPA for 30 min or 90 min (***B***; top and bottom respectively). Dotted white lines indicate the distal edge of the growth cone membrane, lamellipodium is labeled L and the central domain is labeled C on the top, merged image. ***C***, Another example of the superimposed pattern of actin and Ca_V2 staining in a TPA-treated growth cone. Blue arrows point to the central and distal ends of a linear array of Ca_V2 immunoreactive puncta in the lamellipodium. ***D***, A higher power view of the image in ***C*** showing the distal edge of the growth cone.

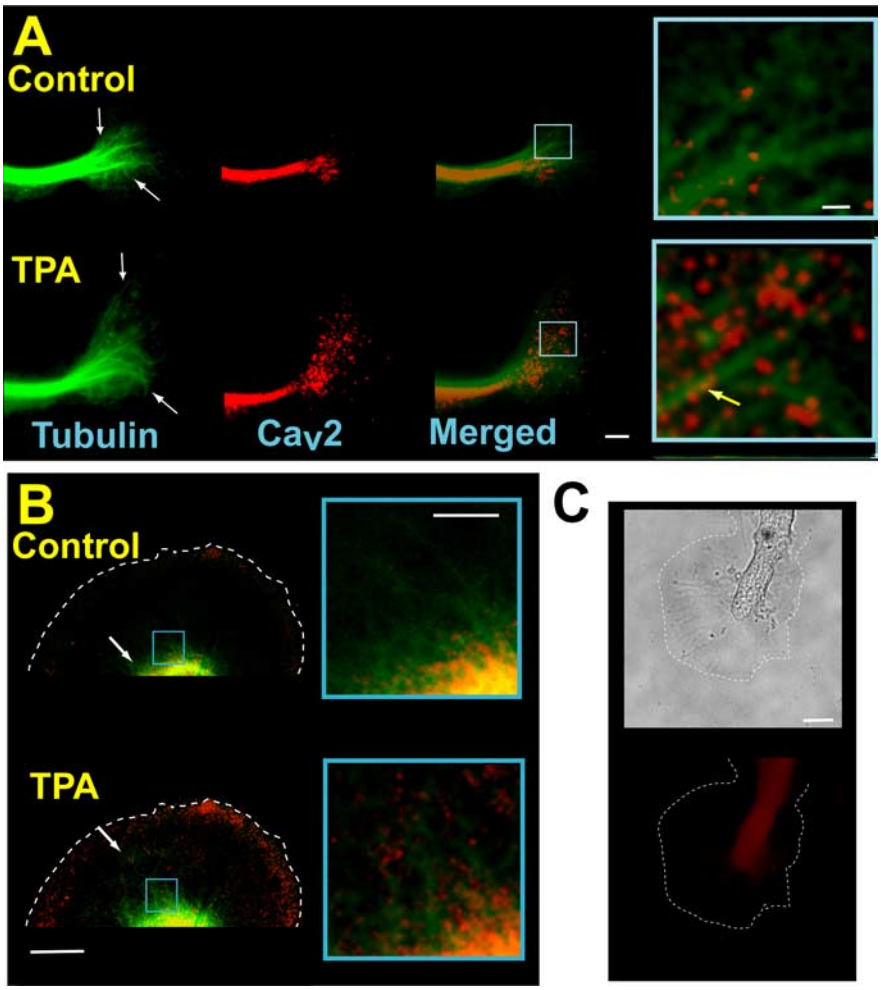

Figure 6. Ca_V2 channels move along microtubules into the distal lamellipodium in live neurons. ***A***, Images of a growth cone in a live neuron treated with green fluorescent tubulin tracker, and injected with fluorescently tagged-antibody against the intracellular epitope of Ca_V2 (red fluorescence). The top shows the tubulin and Ca_V2 staining and superimposed images of both signals before treatment with TPA. White arrows indicate the extent of detectable microtubule staining. The area within the blue box in the merged image is magnified in the inset at right. The bottom shows images of the same cell 5 min after exposure to 100 nM TPA. The yellow arrow in the inset shows localization of Ca_V2 puncta along a microtubule. ***B***, Merged images of tubulin tracker and Ca_V2 staining in another neuron injected with fluorescently tagged anti-Ca_V2 antibody before and after exposure to TPA. White arrows indicate extent of detectable microtubule staining. The areas within the blue boxes are magnified in the insets at right and correspond to the junction between the central region and the lamellipodium. ***C***, Phase and fluorescent image of a neuron injected with secondary anti-rabbit Cy3, and treated with 100 nM TPA. Scale bars: ***A–C***, 10 μm; insets, 2 μm.

Interactions with actin influence the behavior and localization of many ion channels (Cantiello, 1995; Furukawa et al., 1996; Levin et al., 1996; Mazzanti et al., 1996; Jing et al., 1997; Nakahira et al., 1998; Shimoni et al., 1999; Shimoni and Rattner, 2001) It is interesting that of the two agents used in this study to disrupt actin filaments, cytochalasin B and latrunculin B, only the latter was capable of inhibiting the increase in calcium current in response to activation of PKC. Differences in the cellular effects of these two agents have been reported previously (Morales et al., 2000; Bricker et al., 2003; Hubchak et al., 2003; Zeidan et al., 2003) and likely reflect the different mode of action of the two agents. Cytochalasins selectively disrupt actin filaments by preventing filament elongation (Morton et al., 2000), whereas latrunculin B sequesters actin monomers (Brozinick et al., 2004), preventing the formation of newly polymerized actin. It therefore seems likely that insertion of Ca_V2 into the plasma membrane requires nucleation of actin monomers into a new polymer, rather than involvement of previously polymerized actin filaments. Activities that result in the process of *de novo* actin polymerization could include PKC-dependent reorganization of the cytoskeleton similar to that reported to occur during exocytosis of neurotransmitter (Bernstein and Bamburg, 1989; Muallem et al., 1995; Lang et al., 2000; Furuyashiki et al., 2002) and insulin-dependent recruitment of glucose transporter 4 (GLUT4) receptors (Omata et al., 2000). PKC-dependent *de novo* actin nucleation on vesicular ion channels may involve molecules such as neural Wiskott-Aldrich syndrome protein, the arp2/3 complex, and Rho GTPases (Miki and Takenawa, 2003).

Another possible effect of activation of PKC is to depolymerize the established actin filament network, removing a barrier to vesicle trafficking and docking, and thereby promoting translocation (Muallem et al., 1995). These actions of PKC would not necessarily be at odds with the process of *de novo* polymerization of actin. Both processes may occur during fusion events. In addition, the combined actions of microtubules and actin may be important for the proper localization of the intracellular channel before insertion. Although nocodazole did not block the insertion of Ca_V2 channels, PKC activation in the presence of this agent preferentially increased plasma membrane Ca_V2 staining on the neurite shaft and central growth cone, although the localization to the distal growth cone edge was disrupted. Nocodazole disorganizes microtubule tracks, possibly contributing to this mislocalization.

Changes in neuronal excitability and neuropeptide release from adult bag cell neurons are evoked by brief stimulation of an afferent input from the head ganglia. The changes in excitability endure for ~30 min, but the release of neuropeptide can occur for over 1 h after the initial stimulation (Wayne et al., 1999), suggesting that long-term changes in the architecture of the sites of neuropeptide release at the axon endings may occur. Onset of the change in excitability (afterdischarge) is associated with the activation of PKC (DeRiemer et al., 1985; Strong et al., 1987; Knox et al., 1992; White et al., 1998; Wayne et al., 1999). In neuronal growth cones, activation of PKC results in extension of microtubules into the actin-rich lamellipodial region (Kabir et al., 2001), consistent with the possibility that such extension permits insertion of membrane proteins at the distal edge. In the BCNs stimulation of an afterdischarge leads to the activation of multiple protein kinases. These kinases act in concert to produce a structural modification of the tips of neurites, rapidly transforming them into bulbous endings filled with neuropeptide granules adjacent to the newly inserted calcium channels (Knox et al., 1992; Azhderian et al., 1994). These newly restructured sites are likely to represent new sites of release for the peptide transmitters of these neurons. Our observations suggest that PKC may regulate the trafficking of the Ca_V2 calcium channels into and out of cell membranes in

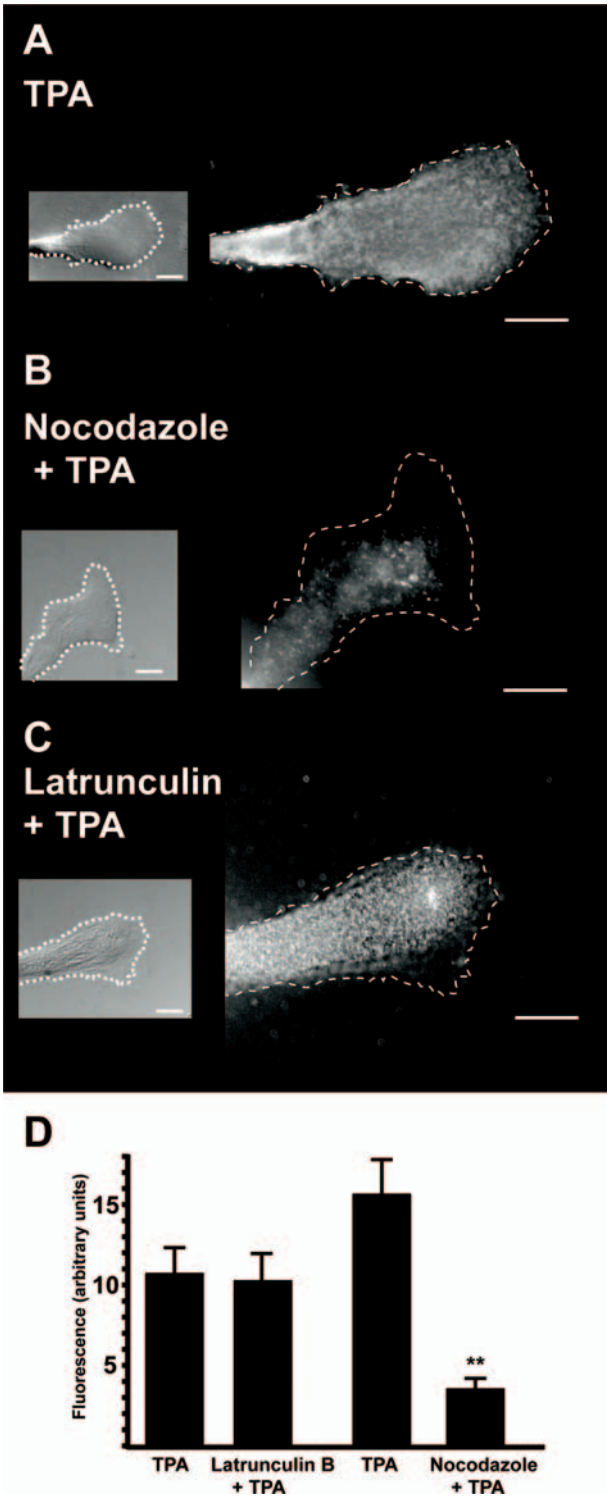

Figure 7. Nocodazole, but not latrunculin B, prevents movement of Ca_V2 to the distal edge of the lamellipodium after activation of PKC. ***A–C***, Phase contrast images of growth cones and fluorescence immunolocalization of Ca_V2 using an antibody to an intracellular epitope in permeabilized cells in the presence of 100 nM TPA alone (***A***), in response to 100 nM TPA after pretreatment with nocodazole (100 nM for 60 min) (***B***), or in response to 100 nM TPA after pretreatment with latrunculin B (10 μM for 60 min) (***C***). Dotted white lines indicate the distal edge of the lamellipodium. Scale bars, 10 μm. ***D***, Left two bar graphs plot the intensity of anti-Ca_V2 fluorescence at the distal edge of the growth cones in the presence of TPA with and without pretreatment with latrunculin B (10 μM). Data shown are for 10 TPA-treated and 10 TPA/latrunculin-treated neurons isolated from the same bag cell cluster. The right pair of bar graphs plot intensity of anti-Ca_V2 fluorescence at the distal edge of the growth cones in the presence of TPA with and without pretreatment with nocodazole (100 nM). Data shown are for 11 TPA-treated and 11 TPA/nocodazole-treated neurons isolated from the same bag cell cluster. Data represent mean ± SE. $^{**}p < 0.001$.

neurite endings in response to stimuli that alter neurotransmitter release.

Work with *Lymnaea* neurons has demonstrated that Ca_V2 subunits are associated with their β subunits at mature release sites, but that the α and β subunits are uncoupled at the leading edge of growth cones of outgrowing neurites, and that β subunit mRNA can be locally translated in growth cones (Spafford et al., 2004). Interestingly, $Ca_v\beta$ and Ca_V2 α subunits appear to be associated with different cytoskeletal elements in immature growth cones (Spafford et al., 2004). It is tempting to speculate that the association between α and β subunits is regulated by PKC and/or by changes in the association of these subunits with the cytoskeleton. (Spafford et al., 2004).

PKC is activated by stimulation of the input to the BCNs (Wayne et al., 1999) and also by binding of insulin to its receptor, which modulates both ion currents and neurosecretion (Jonas et al., 1996; Sossin et al., 1996). In other cell types, such as adipocytes, the binding of insulin to its receptor activates the translocation of the glucose transporter (GLUT4) from an intracellular vesicle to the plasma membrane (Watson et al., 2004), possibly after rapidly occurring actin remodeling (Muallem et al., 1995; Lang et al., 2000; Tong et al., 2001). The actions of insulin in the nervous system of many species including *Aplysia*, *Drosophila*, *C. elegans*, and rodents have important implications for regulation of metabolism, lifespan, and the normal physiological processes of learning and memory (Skeberdis et al., 2001; Dillin et al., 2002; Hertweck et al., 2004; Corl et al., 2005). In addition, the coordination of the addition of new membrane, modulation of ion currents, and clustering of neurotransmitter-containing vesicles is a general requirement for synapse formation (Ziv and Garner, 2004).

References

Azhderian EM, Kaczmarek LK (1990) Cyclic AMP regulates processing of neuropeptide precursor in bag cell neurons of *Aplysia.* J Mol Neurosci 2:61–70.

Azhderian EM, Hefner D, Lin CH, Kaczmarek LK, Forscher P (1994) Cyclic AMP modulates fast axonal transport in *Aplysia* bag cell neurons by increasing the probability of single organelle movement. Neuron 12:1223–1233.

Baines RA (2003) Postsynaptic protein kinase A reduces neuronal excitability in response to increased synaptic excitation in the *Drosophila* CNS. J Neurosci 23:8664–8672.

Bernstein BW, Bamburg JR (1989) Cycling of actin assembly in synaptosomes and neurotransmitter release. Neuron 3:257–265.

Bricker JL, Chu S, Kempson SA (2003) Disruption of F-actin stimulates hypertonic activation of the BGT1 transporter in MDCK cells. Am J Physiol Renal Physiol 284:F930–F937.

Brozinick Jr JT, Hawkins ED, Strawbridge AB, Elmendorf JS (2004) Disruption of cortical actin in skeletal muscle demonstrates an essential role of the cytoskeleton in glucose transporter 4 translocation in insulin-sensitive tissues. J Biol Chem 279:40699–40706.

Cantiello HF (1995) Role of the actin cytoskeleton on epithelial Na^+ channel regulation. Kidney Int 48:970–984.

Conn PJ, Kaczmarek LK (1989) The bag cell neurons of *Aplysia.* A model for the study of the molecular mechanisms involved in the control of prolonged animal behaviors Mol Neurobiol 3:237–273.

Conn PJ, Strong J, Kaczmarek L (1989a) Inhibitors of protein kinase C prevent enhancement of calcium current and action potentials in peptidergic neurons of *Aplysia.* J Neurosci 9:480–487.

Conn PJ, Strong J, Azhderian E, Nairn A, Greengard P, Kaczmarek L (1989b) Protein kinase inhibitors selectively block phorbol ester- or forskolin-induced changes in excitability of *Aplysia* neurons. J Neurosci 9:473–479.

Cooper J (1987) Effects of cytochalasin and phalloidin on actin. J Cell Biol 105:1473–1478.

Corl AB, Rodan AR, Heberlein U (2005) Insulin signaling in the nervous system regulates ethanol intoxication in *Drosophila* melanogaster. Nat Neurosci 8:18–19.

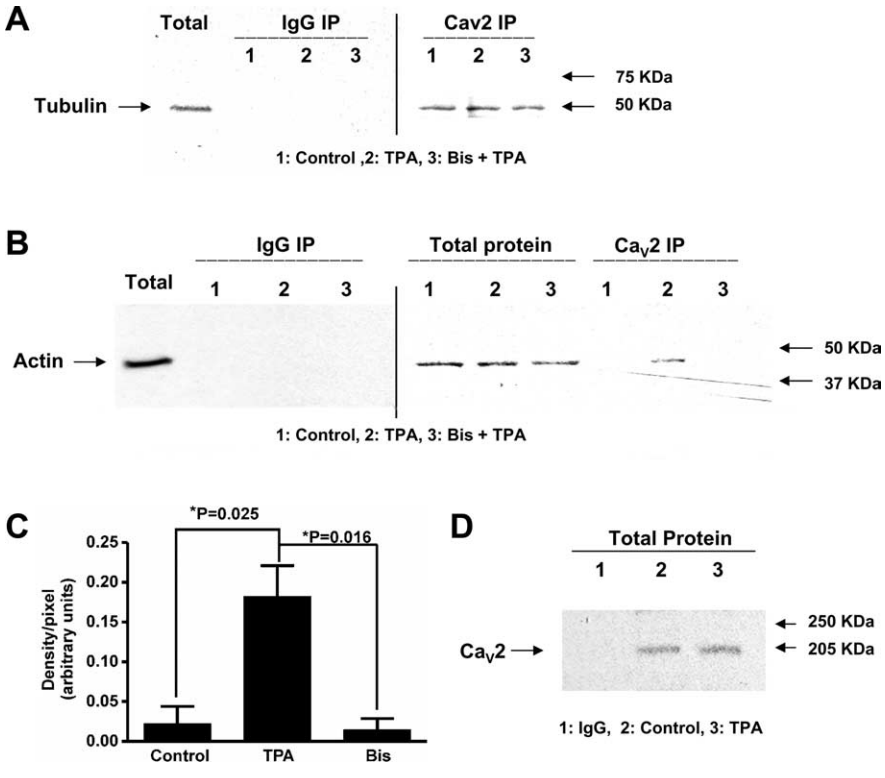

Figure 8. Activation of PKC induces actin to coimmunoprecipitate with Ca_V2 channels. ***A***, After homogenizing bag cell clusters, protein extracts were either subjected directly to SDS-PAGE for immunoblotting with an anti-tubulin antibody (left lane, 40 μg) or subjected to immunoprecipitation using control anti-rabbit IgG antibodies (left lanes 1–3), or using antibodies to the intracellular epitope of Ca_V2 (right lanes 1–3) before immunoblotting with the anti-tubulin antibody. Before homogenization the clusters were incubated for 30 min either in control ASW (1), in ASW containing 100 nM TPA (2), or in ASW with 100 nM TPA in the presence of 1 μM BIS, an inhibitor of PKC (3). ***B***, Actin coimmunoprecipitates with Ca_V2 after activation of protein kinase C. Bag cell protein extracts were either subjected directly to SDS-PAGE for immunoblotting with an anti-actin antibody developed in rabbit (left lane, 100 μg), or an anti-actin antibody developed in mouse (right lanes, labeled total protein, 100 μg each) or were subjected to immunoprecipitation using control anti-mouse IgG antibodies (left lanes, 1–3) or using antibodies to the intracellular epitope of Ca_V2 (*right* lanes marked Ca_V2 IP 1–3) before Western blotting. Lanes 1–3 in each case represent extracts from cells treated with control ASW (1), 100 nM TPA (2) or 100 nM TPA with 1 μM BIS (3). ***C***, Quantification of the effect of TPA on coimmunoprecipitation of Ca_V2 with actin using densitometric analysis ($n = 3$). ***D***, Western blot of Ca_V2 immunoprecipitates from control cells and those exposed to 100 nM TPA demonstrating that activation of PKC does not alter Ca_V2 levels.

DeRiemer SA, Strong JA, Albert KA, Greengard P, Kaczmarek LK (1985) Enhancement of calcium current in *Aplysia* neurones by phorbol ester and protein kinase C. Nature 313:313–316.

Dillin A, Crawford DK, Kenyon C (2002) Timing requirements for insulin/IGF-1 signaling in *C. elegans*. Science 298:830–834.

Eisenstadt M, Goldman JE, Kandel ER, Koike H, Koester J, Schwartz JH (1973) Intrasomatic injection of radioactive precursors for studying transmitter synthesis in identified neurons of *Aplysia* californica. Proc Natl Acad Sci USA 70:3371–3375.

Emoto K, He Y, Ye B, Grueber WB, Adler PN, Jan LY, Jan YN (2004) Control of dendritic branching and tiling by the tricornered-kinase/furry signaling pathway in *Drosophila* sensory neurons. Cell 119:245–256.

Ennion SJ, Evans RJ (2002) Conserved cysteine residues in the extracellular loop of the human P2X(1) receptor form disulfide bonds and are involved in receptor trafficking to the cell surface. Mol Pharmacol 61:303–311.

Fadool DA, Tucker K, Perkins R, Fasciani G, Thompson RN, Parsons AD, Overton JM, Koni PA, Flavell RA, Kaczmarek LK (2004) Kv1.3 channel gene-targeted deletion produces "super-smeller mice" with altered glomeruli, interacting scaffolding proteins, and biophysics. Neuron 41:389–404.

Fisher TE, Kaczmarek LK (1990) The regulation of excitability by second messengers and protein kinases in peptidergic neurons of *Aplysia.* Adv Second Messenger Phosphoprotein Res 24:41–44.

Forscher P, Kaczmarek L, Buchanan J, Smith S (1987) Cyclic AMP induces changes in distribution and transport of organelles within growth cones of *Aplysia* bag cell neurons. J Neurosci 7:3600–3611.

Furukawa T, Yamane T, Terai T, Katayama Y, Hiraoka M (1996) Functional linkage of the cardiac ATP-sensitive K^+ channel to the actin cytoskeleton. Pflugers Arch 431:504–512.

Furuyashiki T, Arakawa Y, Takemoto-Kimura S, Bito H, Narumiya S (2002) Multiple spatiotemporal modes of actin reorganization by NMDA receptors and voltage-gated Ca^{2+} channels. Proc Natl Acad Sci USA 99:14458–14463.

Gauthier LR, Charrin BC, Borrell-Pages M, Dompierre JP, Rangone H, Cordelieres FP, De Mey J, MacDonald ME, Lessmann V, Humbert S, Saudou F (2004) Huntingtin controls neurotrophic support and survival of neurons by enhancing BDNF vesicular transport along microtubules. Cell 118:127–138.

Hertweck M, Gobel C, Baumeister R (2004) *C. elegans* SGK-1 is the critical component in the Akt/PKB kinase complex to control stress response and life span. Developmental Cell 6:577–588.

Huang H, Rao Y, Sun P, Gong L-W (2002) Involvement of actin cytoskeleton in modulation of Ca^{2+}-activated K^+ channels from rat hippocampal CA1 pyramidal neurons. Neurosci Lett 332:141–145.

Huang JD, Brady ST, Richards BW, Stenoien D, Resau JH, Copeland NG, Jenkins NA (1999) Direct interaction of microtubule- and actin-based transport motors. Nature 397:267–270.

Hubchak SC, Runyan CE, Kreisberg JI, Schnaper HW (2003) Cytoskeletal rearrangement and signal transduction in TGF-beta1-stimulated mesangial cell collagen accumulation. J Am Soc Nephrol 14:1969–1980.

Jing J, Peretz T, Singer-Lahat D, Chikvashvili D, Thornhill WB, Lotan I (1997) Inactivation of a voltage dependent K^+ Channel by beta Subunit. Modulation by a phosphorylation-dependent interaction between the distal C terminus of alpha subunit and cytoskeleton. J Biol Chem 272:14021–14024.

Jonas EA, Knox RJ, Kaczmarek LK, Schwartz JH, Solomon DH (1996) Insulin receptor in *Aplysia* neurons: characterization, molecular cloning, and modulation of ion currents. J Neurosci 16:1645–1658.

Jonas EA, Knox RJ, Smith TC, Wayne NL, Connor JA, Kaczmarek LK (1997) Regulation by insulin of a unique neuronal Ca^{2+} pool and of neuropeptide secretion. Nature 385:343–346.

Kabir N, Schaefer AW, Nakhost A, Sossin WS, Forscher P (2001) Protein kinase C activation promotes microtubule advance in neuronal growth cones by increasing average microtubule growth lifetimes. J Cell Biol 152:1033–1044.

Kaczmarek LK, Strumwasser F (1984) A voltage-clamp analysis of currents underlying cyclic AMP-induced membrane modulation in isolated peptidergic neurons of *Aplysia.* J Neurophysiol 52:340–349.

Kaczmarek LK, Jennings KR, Strumwasser F, Nairn AC, Walter U, Wilson FD, Greengard P (1980) Microinjection of catalytic subunit of cyclic AMP-dependent protein kinase enhances calcium action potentials of bag cell neurons in cell culture. Proc Natl Acad Sci USA 77:7487–7491.

Keenan C, Kelleher D (1998) Protein kinase C and the cytoskeleton. Cell Signal 10:225–232.

Knox RJ, Quattrocki EA, Connor JA, Kaczmarek LK (1992) Recruitment of Ca^{2+} channels by protein kinase C during rapid formation of putative neuropeptide release sites in isolated *Aplysia* neurons. Neuron 8:883–889.

Lang T, Wacker I, Wunderlich I, Rohrbach A, Giese G, Soldati T, Almers W (2000) Role of actin cortex in the subplasmalemmal transport of secretory granules in PC-12 cells. Biophys J 78:2863–2877.

Levin G, Chikvashvili D, Singer-Lahat D, Peretz T, Thornhill WB, Lotan I (1996) Phosphorylation of a K^+ channel alpha subunit modulates the

inactivation conferred by a beta subunit. Involvement of cytoskeleton. J Biol Chem 271:29321–29328.
Levina N, Lew R, Heath I (1994) Cytoskeletal regulation of ion channel distribution in the tip-growing organism *Saprolegnia ferax*. J Cell Sci 107:127–134.
Lin CH, Forscher P (1993) Cytoskeletal remodeling during growth cone-target interactions. J Cell Biol 121:1369–1383.
Lin YF, Raab-Graham K, Jan YN, Jan LY (2004) NO stimulation of ATP-sensitive potassium channels: Involvement of Ras/mitogen-activated protein kinase pathway and contribution to neuroprotection. Proc Natl Acad Sci USA 101:7799–7804.
Mazzanti M, Assandri R, Ferroni A, DiFrancesco D (1996) Cytoskeletal control of rectification and expression of four substates in cardiac inward rectifier K^+ channels. FASEB J 10:357–361.
Miki H, Takenawa T (2003) Regulation of actin dynamics by WASP family proteins. J Biochem (Tokyo) 134:309–313.
Morales M, Colicos MA, Goda Y (2000) Actin-dependent regulation of neurotransmitter release at central synapses. Neuron 27:539–550.
Morton WM, Ayscough KR, McLaughlin PJ (2000) Latrunculin alters the actin-monomer subunit interface to prevent polymerization. Nat Cell Biol 2:376–378.
Muallem S, Kwiatkowska K, Xu X, Yin H (1995) Actin filament disassembly is a sufficient final trigger for exocytosis in nonexcitable cells. J Cell Biol 128:589–598.
Nakahira K, Matos MF, Trimmer JS (1998) Differential interaction of voltage-gated K^+ channel beta-subunits with cytoskeleton is mediated by unique amino terminal domains. J Mol Neurosci 11:199–208.
Nakhost A, Forscher P, Sossin WS (1998) Binding of protein kinase C isoforms to actin in *Aplysia.* J Neurochem 71:1221–1231.
Nakhost A, Kabir N, Forscher P, Sossin WS (2002) Protein kinase C isoforms are translocated to microtubules in neurons. J Biol Chem 277:40633–40639.
Nick TA, Kaczmarek LK, Carew TJ (1996) Ionic currents underlying developmental regulation of repetitive firing in *Aplysia* bag cell neurons. J Neurosci 16:7583–7598.
Omata W, Shibata H, Li L, Takata K, Kojima I (2000) Actin filaments play a critical role in insulin-induced exocytotic recruitment but not in endocytosis of GLUT4 in isolated rat adipocytes. Biochem J 346:321–328.
Prahlad V, Helfand B, Langford G, Vale R, Goldman R (2000) Fast transport of neurofilament protein along microtubules in squid axoplasm. J Cell Sci 113:3939–3946.
Schubert T, Akopian A (2004) Actin filaments regulate voltage-gated ion channels in salamander retinal ganglion cells. Neuroscience 125:583–590.
Shimoni Y, Rattner JB (2001) Type 1 diabetes leads to cytoskeleton changes that are reflected in insulin action on rat cardiac K^+ currents. Am J Physiol Endocrinol Metab 281:E575–E585.
Shimoni Y, Ewart HS, Severson D (1999) Insulin stimulation of rat ventricular K^+ currents depends on the integrity of the cytoskeleton. J Physiol (Lond) 514:735–745.
Skeberdis VA, Lan JY, Zheng X, Zukin RS, Bennett MVL (2001) Insulin promotes rapid delivery of N-methyl-D-aspartate receptors to the cell surface by exocytosis. Proc Natl Acad Sci USA 98:3561–3566.
Smith PR, Stoner LC, Viggiano SC, Angelides KJ, Benos DJ (1995) Effects of vasopressin and aldosterone on the lateral mobility of epithelial Na^+ channels in A6 renal epithelial cells. J Membr Biol 147:195–205.
Sossin WS, Chen CS, Toker A (1996) Stimulation of an insulin receptor activates and down-regulates the Ca^{2+}-Independent protein kinase C, Apl II, through a wortmannin-sensitive signaling pathway in *Aplysia*. J Neurochem 67:220–228.
Spafford JD, Chen L, Feng ZP, Smit AB, Zamponi GW (2003) Expression and modulation of an invertebrate presynaptic calcium channel alpha1 subunit homolog. J Biol Chem 278:21178–21187.
Spafford JD, van Minnen J, Larsen P, Smit AB, Syed NI, Zamponi GW (2004) Uncoupling of calcium channel alpha1 and beta subunits in developing neurons. J Biol Chem 279:41157–41167.
Spafford JD, Dunn T, Smit AB, Syed NI, Zamponi GW (2006) In vitro characterization of L-type calcium channels and their contribution to firing behavior in invertebrate respiratory neurons. J Neurophysiol 95:42–52.
Strong JA, Fox AP, Tsien RW, Kaczmarek LK (1987) Stimulation of protein kinase C recruits covert calcium channels in *Aplysia* bag cell neurons. Nature 325:714–717.
Tong P, Khayat ZA, Huang C, Patel N, Ueyama A, Klip A (2001) Insulin-induced cortical actin remodeling promotes GLUT4 insertion at muscle cell membrane ruffles. J Clin Invest 108:371–381.
Tulsi RS, Coggeshall RE (1971) Neuromuscular junctions on the muscle cells in the central nervous system of the leech, *Hirudo medicinalis*. J Comp Neurol 141:1–15.
Watson RT, Kanzaki M, Pessin JE (2004) Regulated membrane trafficking of the insulin-responsive glucose transporter 4 in adipocytes. Endocr Rev 25:177–204.
Wayne NL, Lee W, Kim YJ (1999) Persistent activation of calcium-activated and calcium-independent protein kinase C in response to electrical after-discharge from peptidergic neurons of *Aplysia.* Brain Res 834:211–213.
White BH, Kaczmarek LK (1997) Identification of a vesicular pool of calcium channels in the bag cell neurons of *Aplysia* californica. J Neurosci 17:1582–1595.
White BH, Nick TA, Carew TJ, Kaczmarek LK (1998) Protein Kinase C regulates a vesicular class of calcium channels in the bag cell neurons of *Aplysia.* J Neurophysiol 80:2514–2520.
Wilson GF, Kaczmarek LK (1993) Mode-switching of a voltage-gated cation channel is mediated by a protein kinase A-regulated tyrosine phosphatase. Nature 366:433–438.
Yano H, Chao MV (2004) Mechanisms of neurotrophin receptor vesicular transport. J Neurobiol 58:244–257.
Zeidan A, Nordstrom I, Albinsson S, Malmqvist U, Sward K, Hellstrand P (2003) Stretch-induced contractile differentiation of vascular smooth muscle: sensitivity to actin polymerization inhibitors. Am J Physiol Cell Physiol 284:C1387–C1396.
Ziv NE, Garner CC (2004) Cellular and molecular mechanisms of presynaptic assembly. Nat Rev Neurosci 5:385–399.